Development of a new method for neutrino interaction measurements with the DUNE-PRISM detector

Jeremy Atkinson
University of Birmingham
Supervisor: Dr. C.F. Vilela

Summer 2021
21st of June - 3rd of September

Abstract

This report presents the work towards a data-driven technique to investigate neutrino cross-section measurements. By linearly combining neutrino flux spectra measured at different off-axis positions at the DUNE Near Detector, and by finding the correct coefficients, Gaussian target flux spectra can be produced. The results outlined in the DUNE ND CDR [1] were successfully reproduced. This new method allows for previously inaccessible variables to be investigated by extending the neutrino flux matrix to take into account lepton energy and angle. This was first applied to the energy transferred to the nucleus, $E_\nu - E_l$, before being generalised to arbitrary functions. Other new variables for which this was applied were the elasticity of the interaction, $\frac{E_l}{E_\nu}$, and the Q^2 value. By comparing the coefficients for $E_\nu - E_l$ to simulated data, it was shown that this method can successfully identify the relevant interaction modes at a given energy transfer, which could allow for neutrino cross-section measurements and neutrino interaction model improvements.

Contents

1 DUNE and DUNE-PRISM

The Deep Underground Neutrino Experiment (DUNE) is a neutrino oscillation experiment based in the USA, currently under development. A neutrino beam will be produced at the Fermi National Accelerator Laboratory (Fermilab) in Batavia, Illinois, with a Near Detector (ND) on site, and a Far Detector (FD) approximately 1300 km away at the Sanford Underground Research Facility (SURF) in Lead, South Dakota, around 1.5 km underground. To be able to understand the results at the FD, the characteristics of the neutrino beam as it leaves Fermilab need to investigated, hence the requirement for the ND, located 574 m from the neutrino beam source. It is designed as a suite of three detectors, one of which remains on axis at all times, and two which can move up to 30.5 m off-axis, as shown in Figure 1. This project focuses on one of these movable detectors, the ND-LAr, a liquid argon time projection chamber (LArTPC), and its role in DUNE-PRISM (DUNE Precision Reaction-Independent Spectrum Measurement) [1]. The neutrino flux spectrum changes as it is measured at different off-axis angles (Figure 2a).

Typical scattering experiments, such as electron scattering off nuclei (Figure 2b), can be powerful probes of nuclear models if the initial and final states are well known. For conventional neutrino experiments, the neutrino energy is not well known, so it is necessary to rely only on the reconstruction of final state hadrons; this is limited as some go undetected, such neutrons. By creating linear combinations of the varying neutrino flux spectra to give Gaussian neutrino energy spectra, this effectively allows for the control of the initial state of the neutrinos, leading to data-driven investigations of neutrino cross-sections. Current neutrino models can therefore be tested, and a better understanding of neutrino interactions with matter can be developed.

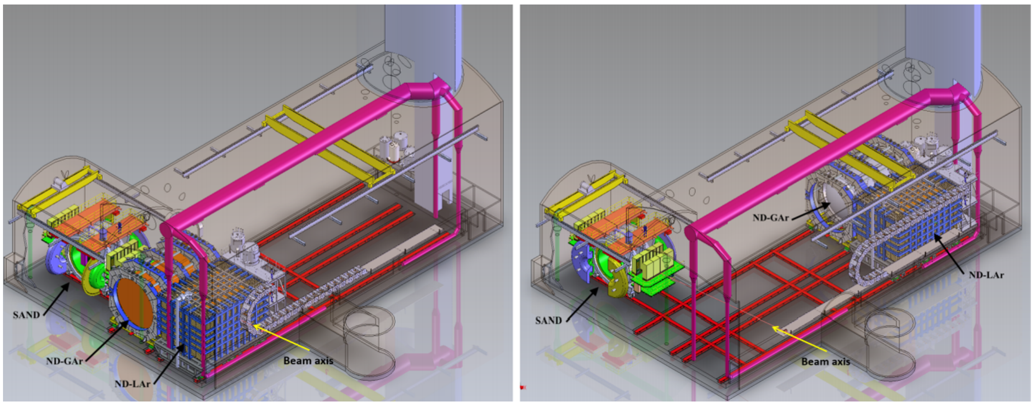

Figure 1: The ND detector suite schematic, showing the stationary SAND (System for on-Axis Neutrino Detection), and the movable ND-GAr (ND gaseous argon TPC) and ND-LAr in both the on-axis position and an off-axis position [1].

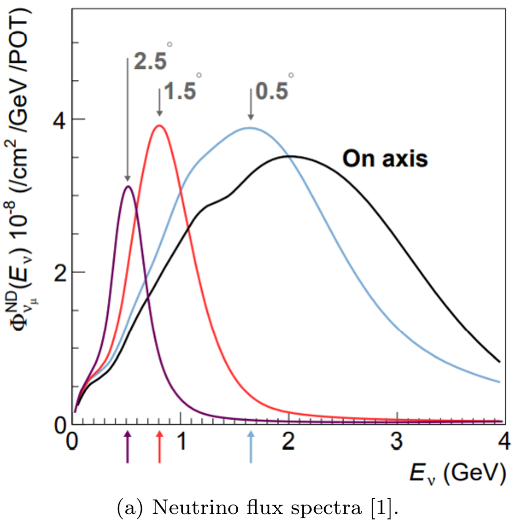

(a) Neutrino flux spectra [1].

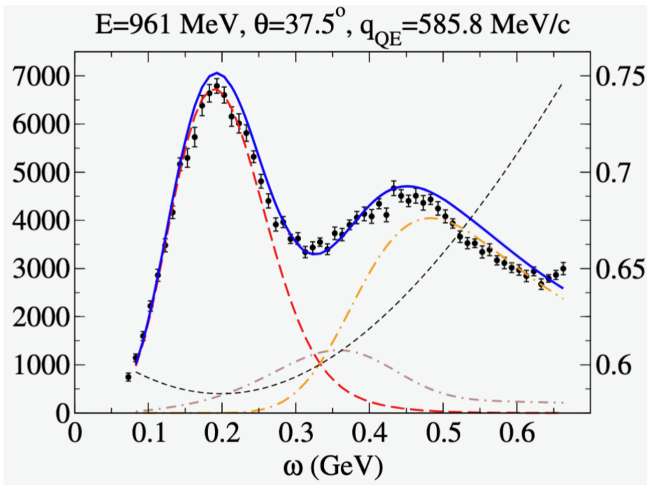

(b) Electron scattering [2].

Figure 2: (a) The neutrino flux spectra at different off-axis angles. (b) An example of an electron-nucleus scattering plot. Different interaction modes are shown by the dashed lines, whereas the total number of events at each energy transfer to the nucleus (ω) is shown by the fitted solid blue curve.

2 Project Goal

The primary goal of this project was to investigate DUNE-PRISM linear combinations using final state lepton variables to allow for neutrino cross-section measurements as a function of previously inaccessible variables, analogous to the electron-scattering case, such as the energy and momentum transferred from the neutrino to the nucleus.

3 Project Development

3.1 First steps

The original flux matrix, `oa_flux`, Figure 3a, had 800 bins in neutrino energy, E_ν, from 0 to 8 GeV, and 58 bins in off-axis angle, d_{OA}, from -0.5 to 57.5 mrad. The target flux should therefore also be of dimension E_ν. A set of coefficients, of dimension d_{OA}, needed to be found to linearly combine the neutrino fluxes at different axis positions to reproduce the target flux - this could be solved as a simple linear algebra problem (Figure 7, step 1). Throughout this project, all target flux curves were Gaussian in shape, with chosen means and widths. The problem is ill-posed, as it doesn't have a unique solution, so to choose a certain set, Tikhonov regularisation was implemented in this project; this is a type of L2 regularisation. To choose which regularisation strength, λ, to apply, the fitting process was looped over a range of λ values - the residual and solution norms for each λ were calculated and plotted against each other to produce an L-curve, as shown in Figure 4a [3]. From this, the point of maximum curvature was found (Figure 4b), and the corresponding λ is selected. A separate file, `regularisation.py`, containing the relevant function was created, and is called when regularisation strength optimisation is required. It is worth noting that despite the theory behind this technique being valid, and ongoing investigations throughout the project's duration, there are still issues when implementing it for variables more complex than simply E_ν. The L-curves often plateaus rather than producing the signature elbow, resulting in a flawed method when attempting regularisation strength optimisation. This would require further development to fully perfect this method.

These calculations have been previously performed in the DUNE Near Detector Conceptual Design Report (CDR) (Figure 5a), and the first steps of this investigation were to reproduce these results (Figure 5b). This was done successfully for a range of mean energies and widths.

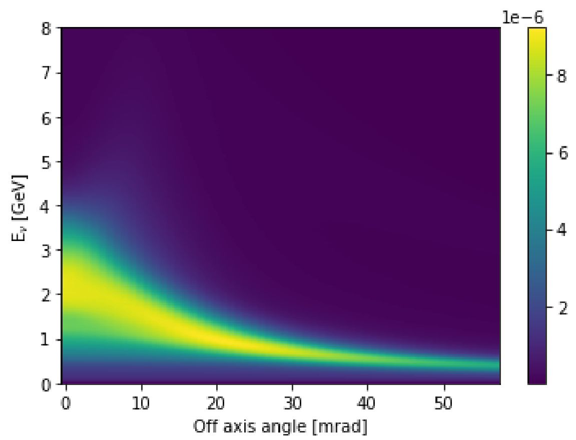

(a) Neutrino flux matrix.

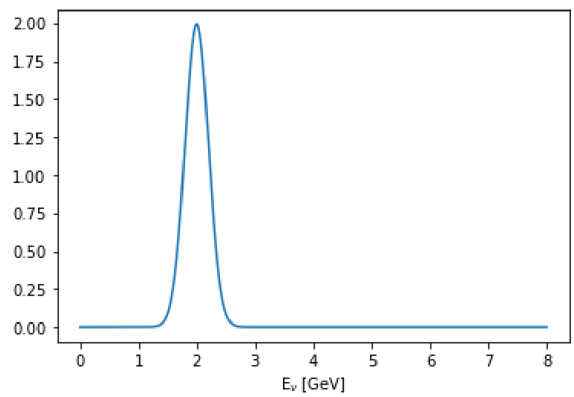

(b) Target flux.

Figure 3: (a) The original off-axis neutrino flux matrix. (b) An example Gaussian target flux with a mean of 2 GeV and a width of 0.2 GeV.

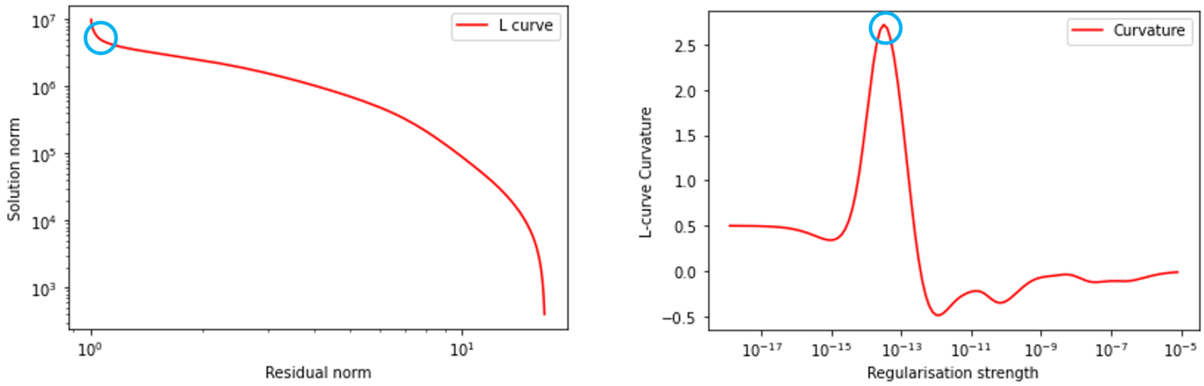

(a) L-curve.

(b) L-curve curvature.

Figure 4: (a) The L-curve produced for a 1 GeV mean, 0.1 GeV width, Gaussian target flux. The signature elbow can be seen (circled in blue), where the point with maximum curvature indicates the optimal value for λ. (b) The curvature of the L-curve in 4a, with a clear peak (circled in blue).

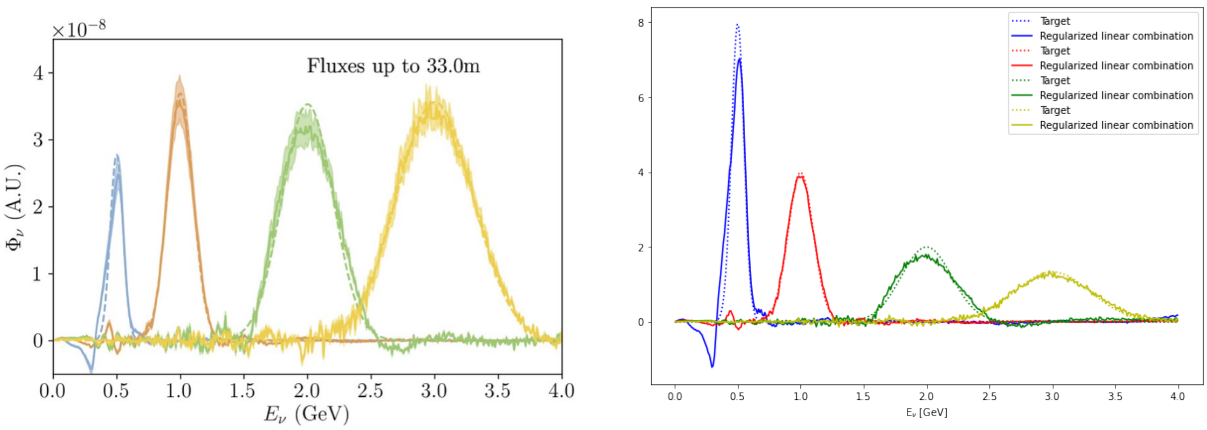

(a) CDR linear combinations [1].

(b) Reproduction of CDR combinations.

Figure 5: (a) The target fluxes and reconstruction using the linear combination method for Gaussian targets with means 0.5, 1.0, 2.0 and 3.0 GeV, with widths 10% of the mean, found in the CDR. (b) Original reproductions of the CDR results achieved in this project.

3.2 Lepton kinematics

The project was then developed by bringing in variables from the lepton kinematics. Once an incident neutrino interacts with the material in the detector, a corresponding lepton is produced (Figure 6). The energy and momentum of the lepton are expected to be well reconstructed in the DUNE ND, giving two key variables - the lepton energy, E_l, and the lepton angle, θ_l, as shown in Figure 6. These allow for further variables to be determined: the energy transferred to the nucleus, $E_\nu - E_l$; the elasticity of the interaction, $\frac{E_l}{E_\nu}$; and the Q^2 value.

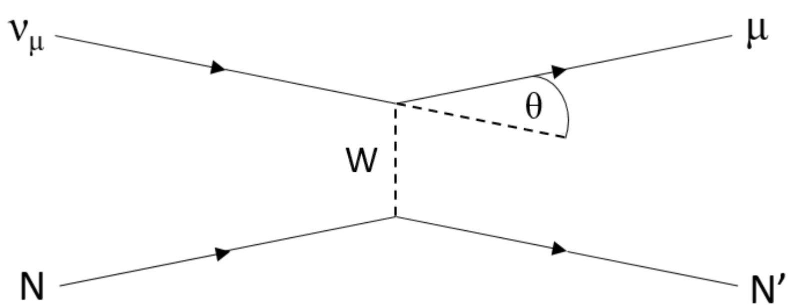

Figure 6: Feynman diagram of the neutrino interaction with a nucleus, with the lepton angle θ shown.

3.3 Lepton energy and the Megamatrix

The initial challenge was to create a new, larger flux matrix, dubbed the "megamatrix", that would incorporate the lepton energy. An initial approach was to simply repeat the original flux matrix for every lepton energy, extending the d_{OA} dimension n times, n being the number of lepton energies considered (Figure 7, step 2). This would in turn extend the coefficient array to also have dimensions $n \times d_{OA}$. To investigate new variables, the y-dimension of the megamatrix also needed to be modified. The first variable chosen to be investigated was the energy transfer $E_\nu - E_l$, as this was the simplest to work with. To achieve this, each time `oa_flux` was repeated, it was shifted down by the value of E_l. This resulted in a y-dimension of $E_\nu - E_l$ (Figure 7, steps 3 and 4).

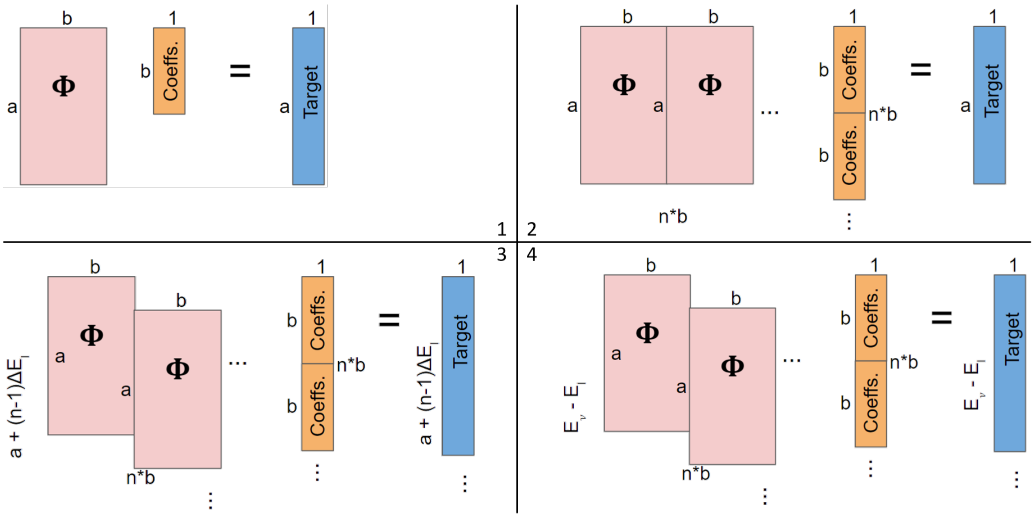

Figure 7: The four stages of the megamatrix production logic in the case of $E_\nu - E_l$. Step 1 is the original linear algebra problem. Step 2 shows the repetition of the neutrino flux matrix for every E_l investigated. Steps 3 and 4 then are the extension of the megamatrix into the $E_\nu - E_l$ dimension. Key: a = E_ν; b = d_{OA}; n = number of E_l investigated; ΔE_l = size of E_l steps.

To minimise the amount of computation required as the megamatrix becomes larger, the `oa_flux` was compressed to have a coarser binning. This was easily achieved by summing nearby bins. In the y-dimension, the neutrino energy bins can be compressed by various even amounts. In the x-dimension, the off-axis angle can only be compressed once to 29 bins rather than 58. In the majority of the results detailed in this paper, it can be assumed the flux matrix used in the megamatrix production has a compression set as 200 neutrino energy bins and 29 off-axis angle bins - if this is not the case, it will be stated. A separate file, `compression.py`, containing the relevant function was created, and is called when a flux matrix needs to be compressed.

The lepton energy range investigated was limited between 0 and 2 GeV (comparable to the electron scattering plot shown in Figure 2b), and was finely binned in 0.1 GeV steps. It should be noted that the unphysical region $E_l < m_\mu$ was not removed - this should be corrected on later work. When first creating the megamatrix, the lepton energy spread used was assumed to be in an array of equal steps. However, this is unrealistic as lepton energies measured will lie on a continuous spectrum. To solve this issue, in every bin, a random number (using a uniform distribution in each bin) was used to shift `oa_flux` down, changing bin to bin. This process was repeated multiple times in a loop, summing all of the total megamatrices togethers, and then divided by the number of loops to calculate an average megamatrix. This had the results of producing a megamatrix with approximately even steps, but smeared in the y-dimension, (Figure 8). This process was used for all new variables investigated. A separate file, `megamatrix.py`, containing the relevant function was created, and is called when megamatrix production is performed.

By expanding the dimensions of the flux matrix to create the megamatrix, an adjustment to the target flux dimension was required. This was straightforward, as the target is of the same dimension as the megamatrix y-dimensions - in this case, also $E_\nu - E_l$ (Figure 7, step 4). This was adjusted for each new variable investigated.

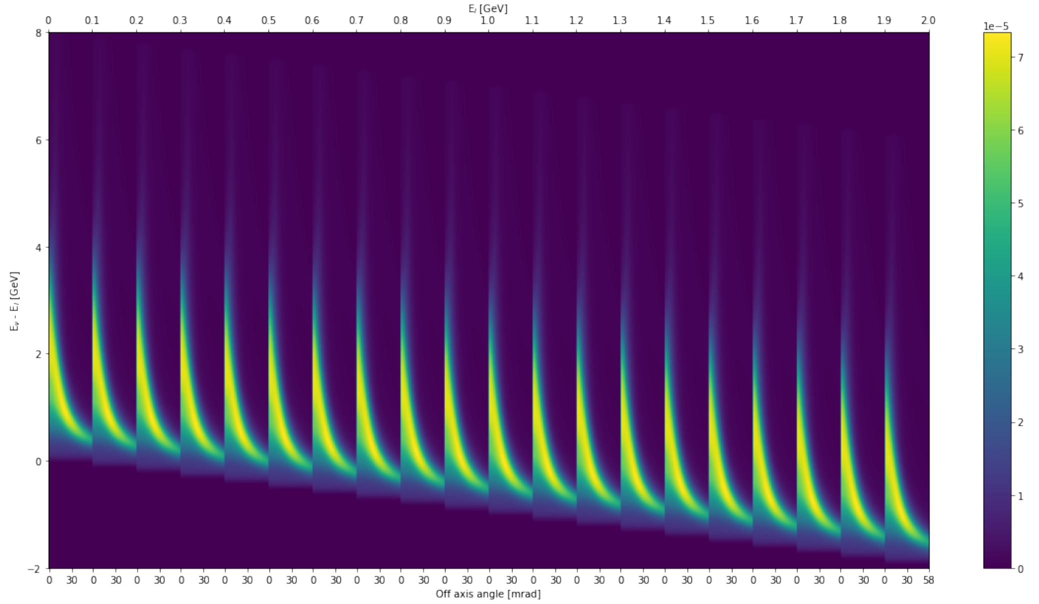

Figure 8: The megamatrix for the energy transfer variable $E_\nu - E_l$, in the lepton energy range 0 to 2 GeV in 0.1 GeV bins. The lepton energy in each bin has been randomised and averaged over 1000 runs.

3.4 Elasticity

To investigate new variables other than $E_\nu - E_l$, the megamatrix function needed to be adapted to take into account other megamatrix structures. It was therefore generalised for alternative cases, taking as arguments: the flux matrix (such as the compressed version of `oa_flux`); a second variable to repeat over (in the case of $E_\nu - E_l$, this was E_l), the energy binning and binning centres of the flux matrix; the function required to calculate the new variable; and the high and low limits of the function. The function supplied always takes two arguments itself - the neutrino energy and the second variable.

Using only the neutrino and lepton energies, another new variable investigated was therefore the elasticity of the interaction. This is defined as $\frac{E_l}{E_\nu}$, quantifying the fraction of the energy of the incoming neutrino that is transferred to the outgoing lepton, and ranges from 0 (inelastic) to 1 (elastic). This meant that the new megamatrix for elasticity was within these limits in the y-dimension, and the flux matrix visually changes considerably as it is repeated, rather than simply being shifted down (Figure 9).

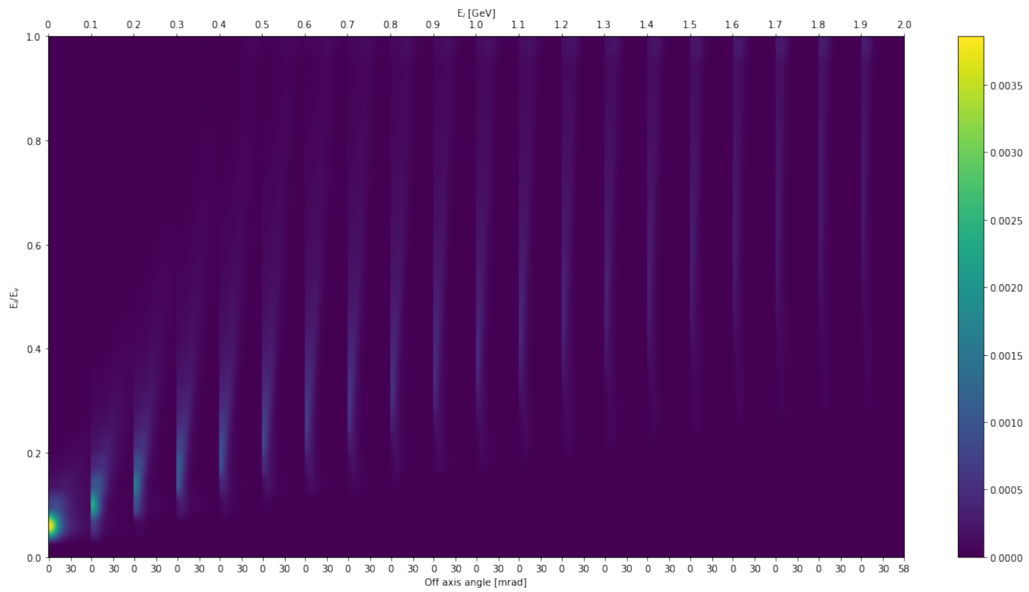

Figure 9: The megamatrix for the elasticity variable $\frac{E_l}{E_\nu}$, in the lepton energy range 0 to 2 GeV in 0.1 GeV bins. The lepton energy in each bin has been randomised and averaged over 1000 runs.

3.5 The Q^2 value

The Q^2 value is another new variable in this investigation, and is defined here as the difference between the four-momenta of the incoming neutrino and the outgoing lepton (Equation 1).

$$Q^2 = \left(\begin{pmatrix} E_\nu \\ \boldsymbol{p_\nu} \end{pmatrix} - \begin{pmatrix} E_l \\ \boldsymbol{p_l} \end{pmatrix} \right)^2 = (E_\nu - E_l)^2 - (\boldsymbol{p_\nu} - \boldsymbol{p_l})^2 \,. \tag{1}$$

For this project, in the context of the neutrinos produced at DUNE and their energy ranges, it can be assumed that $|\boldsymbol{p_\nu}| = E_\nu$, and that the leptons are muons, μ. Q^2 also takes into account the lepton angle. This results in a form for Q^2, written in terms of E_μ and θ_μ, shown in Equation 2. The second variable required as an argument to the function calculating Q^2 is therefore the section in the brackets, which is dependent on both the muon energy and angle. All physical values of Q^2 are negative when using Equation 2, therefore the sign has been switched when plotting.

$$Q^2 = m_\mu^2 + 2E_\nu \left(\sqrt{E_\mu^2 - m_\mu^2} \cos\theta_\mu - E_\mu \right) \tag{2}$$

As expected, the megamatrix for Q^2 takes different forms depending on how the lepton energy and angle vary. Figure 10 shows the effect of changing the energy for a constant angle (left), and vice versa (right). To visualise the effects better, Q was plotted rather than Q^2.

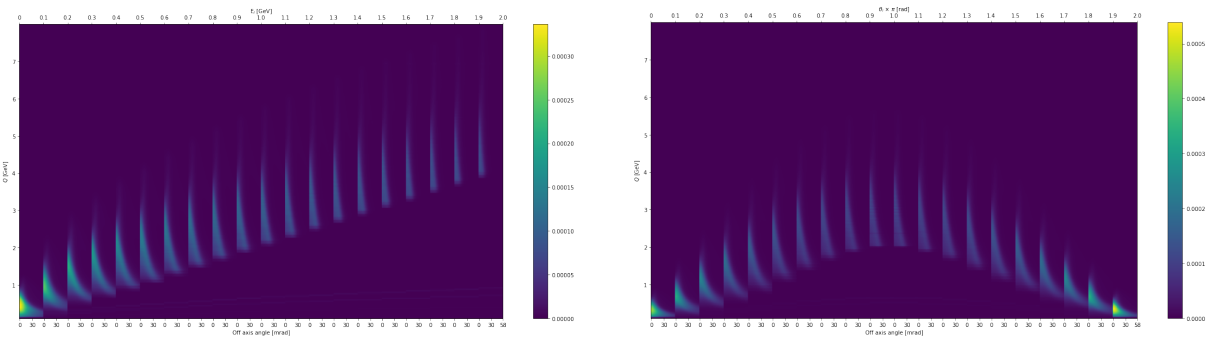

(a) Constant θ_μ, changing E_l. (b) Constant E_l, changing θ_μ.

Figure 10: (a) For a constant θ_μ of π rad, E_l varies between 0 and 2 GeV in 0.1 GeV steps. (b) For a constant E_l of 1 GeV, θ_μ varies between 0 and 2π rad in 0.1π rad steps.

4 Simulated data sets

To support the validity of the method developed in this project, comparisons were made with simulated data sets. The simulated data has a certain distribution of interaction modes (Figure 11a), which can also be binned in a two-dimensional histogram as a function of the new variables (Figure 11c). Investigating the $E_\nu - E_l$ variable, a Gaussian target flux, with a mean of 0.1 Gev and a width of 0.1 GeV, was fitted using the linear combination method described above, with a megamatrix produced by averaging over 1000 randomising runs. The coefficients calculated were then saved and opened in a separate script used to analyse the simulated data. For each simulated event, the lepton energy and off-axis angle were determined and matched to the corresponding coefficient value. The coefficient was then used as a weight for that event. When this weight is applied to the histogram of modes, as shown in Figure 12a, it boosts mode 1 considerably and mode 10 a little, whereas modes 3 and 4 are suppressed. This matches the prediction when looking at Figure 11c, where a large quantity of mode 1, a small quantity of mode 10, and almost no modes 3 and 4 are visible. By applying the weights to a histogram for $E_\nu - E_l$, a Gaussian distribution centred on 0.1 GeV is recovered, resembling the original Gaussian target flux, thus further emphasising the validity of this method.

There are however two things worth noting. Firstly, with the regularisation strength optimisation not working correctly for the $E_\nu - E_l$ variable, a value of 10^{-11} was chosen for these coefficients by looking at different linear combinations and trying sensible values. A different value would yield different results, and should be taken into consideration when interpreting these results. Secondly, the original neutrino flux matrix used to produce the simulated data is similar but not exactly the same as that used in the calculation of coefficients. It is not expected to have major effects on the outcome, but running this process with the same neutrino flux matrix would be ideal.

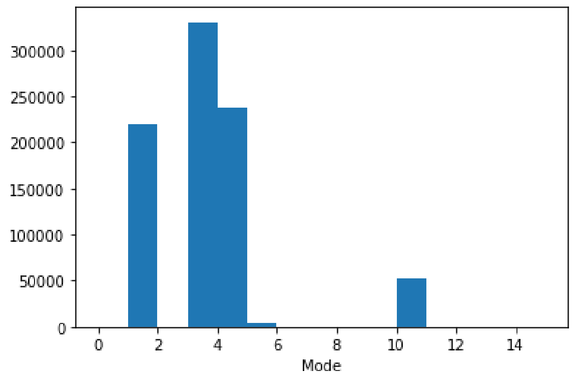

(a) Simulated data interaction modes.

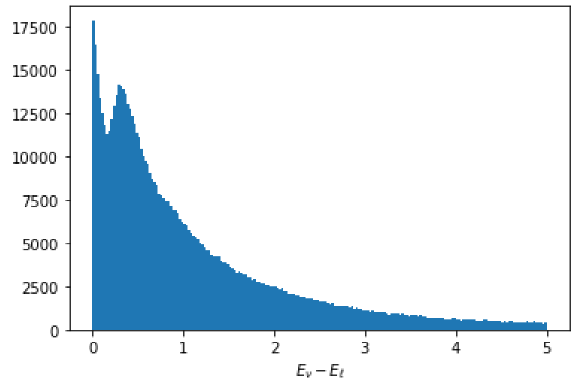

(b) Unweighted distribution of $E_\nu - E_l$.

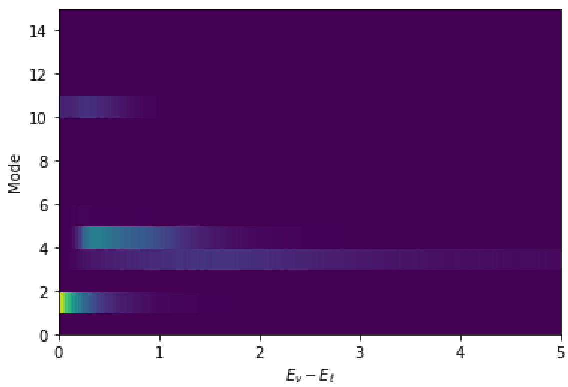

(c) Two-dimensional histogram of the modes and the $E_\nu - E_l$ variable.

Figure 11: (a) Each bin in the histogram represent an interaction mode of the neutrino with matter. The principle modes visible are: Mode 1 - Quasi-elastic scattering; Mode 3 - Deep inelastic scattering; Mode 4 - Resonant scattering; Mode 5 - Coherent scattering; Mode 10 - two-particle-two-hole (2p2h) scattering. (b) The unweighted distribution of events for the $E_\nu - E_l$ variable. (c) A two-dimensional histogram showing the relative number of events for each mode for each $E_\nu - E_l$ energy. For example, at $E_\nu - E_l = 0.1$ GeV, it is expected that mode 1 interactions dominate, with some mode 10 interactions; mode 3 and 4 are much more unlikely.

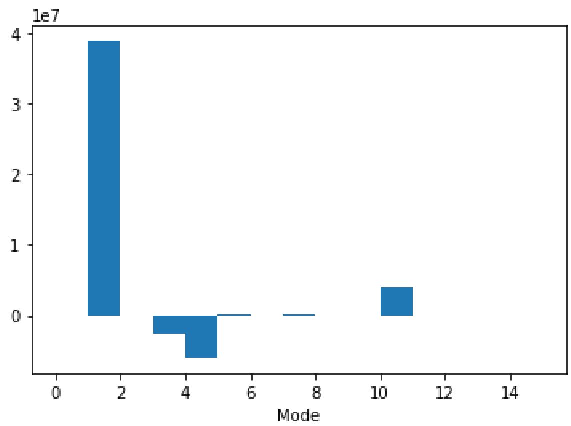

(a) Weighted modes at 0.1 GeV.

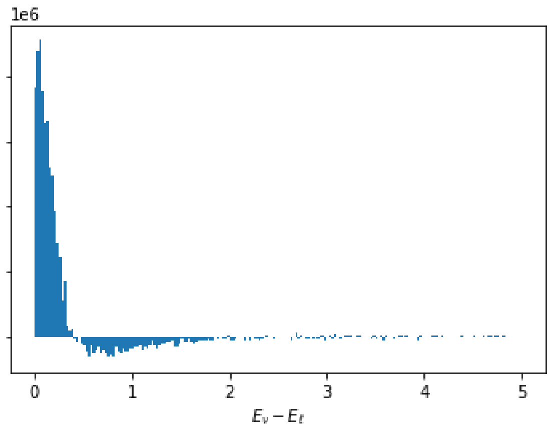

(b) Weighted $E_\nu - E_l$ at 0.1 GeV

Figure 12: Using the coefficients from the linear combination for a Gaussian target flux with a mean and width both of 0.1 GeV, both the modes (a) and the $E_\nu - E_l$ variable (b) can be weighted.

This process was repeated for a Gaussian target flux with a mean of 0.5 GeV and a width of 0.1 GeV, with a regularisation strength of 10^{-9} (which kept the coefficients in a similar range to the previous calculations above). As can be seen in Figures 13a and 13b, most of the weights are negative, but mode 4 is still more prominent than mode 3, as expected from Figure 11a. To visualise this better, an offset of 100, chosen by looking at the typical values of the weights, was added to each weight; the results are shown in Figures 13c and 13d. Despite the Gaussian in Figure 13d being slightly off a 0.5 GeV mean (and the peak around 0.1 GeV), likely due to the different neutrino flux matrices used for the simulated data and the coefficient production, which will have to be resolved in future work, mode 4 is still clearly picked out whereas mode 3 is suppressed, as expected by observing Figure 11c.

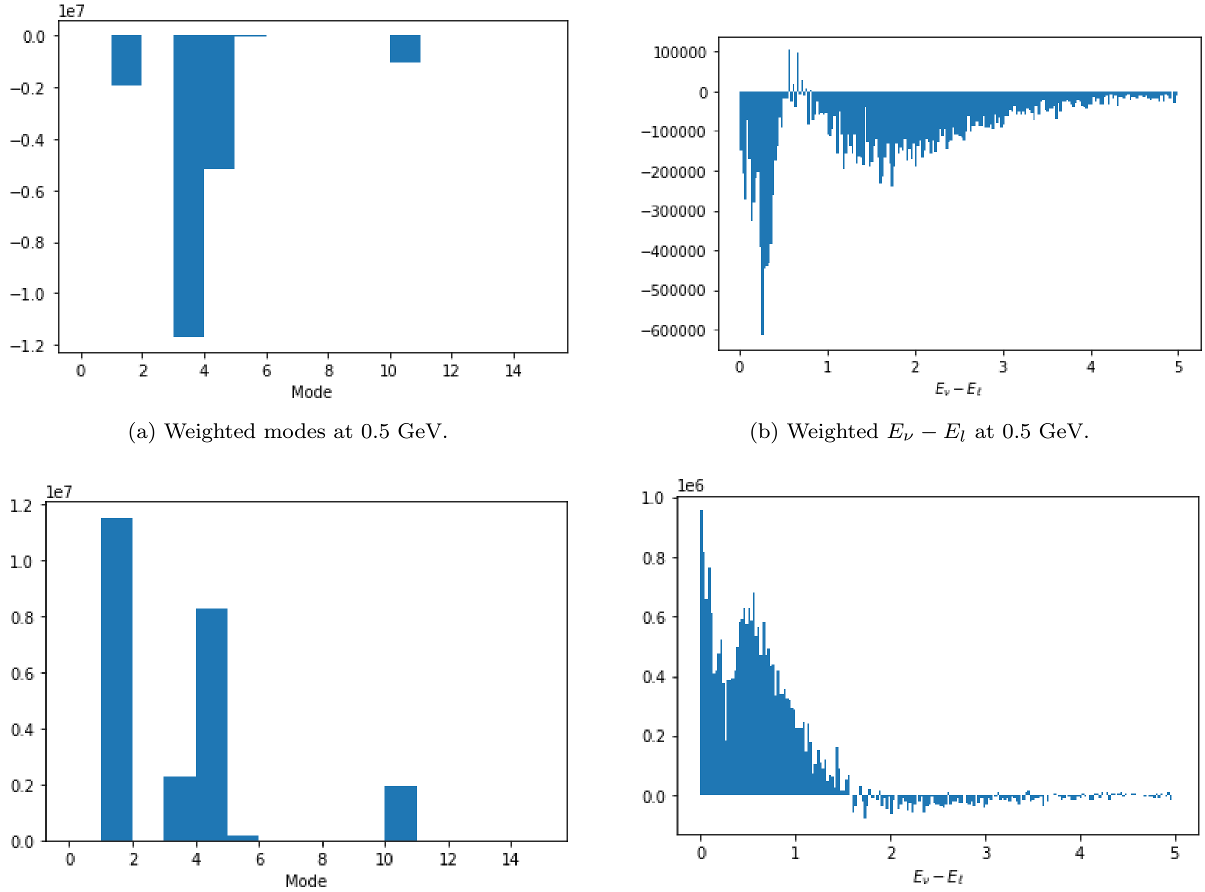

(a) Weighted modes at 0.5 GeV.

(b) Weighted $E_\nu - E_l$ at 0.5 GeV.

(c) Weighted modes at 0.5 GeV, with added offset.

(d) Weighted $E_\nu - E_l$ at 0.5 GeV, with added offset.

Figure 13: Using the coefficients from the linear combination for a Gaussian target flux with a mean of 0.5 GeV and a width of 0.1 GeV, both the modes (a) and the $E_\nu - E_l$ variable (b) can be weighted. To better visualise the plots, an offset of 100 was added to each non-zero weight, as shown in (c) and (d).

5 Conclusion

The construction of megamatrices for $E_\nu - E_l$, $\frac{E_l}{E_\nu}$, and Q^2 were successful, and allowed for the implementation of the DUNE-PRISM linear combination method to reproduce Gaussian target fluxes for the new variables using the lepton kinematics. To further improve this project, the regularisation strength optimisation method should be perfected, to select the best set of coefficients for the linear combination.

The method was successfully applied to simulated data for a 0.1 GeV mean, 0.1 GeV width, Gaussian target flux, where the coefficients calculated for the $E_\nu - E_l$ variable matched predictions made from the simulated data. Further testing of this process for different Gaussian target fluxes with simulated data, along with the required error calculations, would allow for a more refined conclusion on the effectiveness of the technique developed in this project, with this initial investigation already providing promising results.

Acknowledgements

I would like to thank my parents for patiently supporting me throughout the project. Thank you also to my professors at the University of Birmingham (UK), Prof. D.G. Charlton and Prof. K. Nikolopoulos, for helping me in my application for the CERN Summer Student programme. For advice and programming help on L-curves, thank you to Daniel Douglas from Michigan State University (USA). Last but not least, thank you to my incredible supervisor Dr. C.F. Vilela, who has made this project even more exciting and enjoyable than it already was, and for giving me the opportunity to not only present my work to the CERN EP-Nu group, but also internationally to the DUNE-PRISM working group.

References

[1] A. Abed Abud et al. Deep underground neutrino experiment (dune) near detector conceptual design report, 2021.

[2] G.D. Megias, J.E. Amaro, M.B. Barbaro, J.A. Caballero, and T.W. Donnelly. Inclusive electron scattering within the susav2 meson-exchange current approach. *Physical Review D*, 94(1), Jul 2016.

[3] Per Christian Hansen. The l-curve and its use in the numerical treatment of inverse problems. In *InviteComputational Inverse Problems in Electrocardiology*. WIT Press, 2000. InviteComputational Inverse Problems in Electrocardiology ; Conference date: 01-01-2000.